A Novel Schlemm's Canal Scaffold: Histologic Observations

Ian Grierson, PhD, Hady Saheb, MD,† Malik Y. Kahook, MD,‡ Murray A. Johnstone, MD,§ Iqbal I. K. Ahmed, MD,‖ Andrew T. Schieber, MSME,¶ and Carol B. Toris, PhD#*

Purpose: To assess the biocompatibility of a novel implant made of Nitinol (nickel-titanium alloy), designed to improve aqueous humor outflow.

Materials and Methods: In the first arm of biocompatibility testing, microstents were surgically inserted into Schlemm's canal (SC) of 2 non-human primates (NHPs), and a third NHP served as a surgical sham control. After 13 weeks the animals were killed, and the eyes were examined by light and scanning electron microscopy. Two masked investigators evaluated the histology sections. The second arm utilized 8 New Zealand white rabbits; each rabbit received a microstent inserted into the sclera and subconjunctival space by means of passage across the anterior chamber thus providing contact with several representative ocular tissues. The fellow eye of each rabbit underwent a sham procedure without microstent insertion. The rabbits were killed after 26 weeks, and a trained ocular pathologist examined the specimens using light microscopy.

Results: Histologic and scanning electron microscopy analysis of the NHPs demonstrated that the microstents were located in SC. There was no evidence of an acute or chronic inflammatory response, granulation response, or fibrosis in the outflow system or in adjacent tissues. Rabbit eyes showed minimal mononuclear cell infiltration and minimal fibrotic responses at the site of the implants when compared with sham-treated control eyes.

Conclusions: The Hydrus Microstent was associated with minimal inflammation in both NHP and rabbit eyes with extended follow-up. These preclinical studies demonstrate that the Hydrus Microstent appears to have excellent long-term biocompatibility.

Key Words: glaucoma, IOP, human, Schlemm's canal, MIGS, trabecular meshwork, drainage device

(*J Glaucoma* 2013;00:000–000)

BACKGROUND

Surgical lowering of intraocular pressure (IOP) is a critical component in the treatment of glaucoma.[1–3] Trabeculectomy and glaucoma drainage device implantation remain the most commonly performed surgical procedures for the treatment of open-angle glaucoma. These procedures bypass the physiological outflow system of the eye by creating an alternate nonphysiological outflow pathway. Numerous studies have demonstrated good efficacy for these surgical procedures.[1,4,5] However, a high rate of complications has prompted a continuous search for alternative surgeries to treat open-angle glaucoma.[6] There is increasing interest in minimally invasive glaucoma surgeries. Recent publications[7,8] have reviewed the available microinvasive glaucoma surgical (MIGS) options. "MIGS" has been defined as a group of surgical procedures with an ab interno approach that reduce IOP without creating an alternate nonphysiological outflow pathway.

Surgical procedures such as trabeculotomy or the Trabectome procedure attempt to open communication between Schlemm's canal (SC) and the anterior chamber without device implantation.[9–16,12] The removal of the trabecular meshwork (TM), considered to be the site of greatest outflow resistance, provides aqueous humor a direct flow path into SC. The downstream resistance provided by episcleral venous pressure is maintained following SC surgeries thus there is low risk of hypotony and related complications seen with more invasive glaucoma surgeries.[17–22] However, wound healing can affect the patency of unsupported TM openings. More recently, several glaucoma implants have been designed to maintain a fluid pathway into SC without physical removal of the TM.[23–27] However, devices designed for implantation into SC have been limited by the lack of available materials with suitable properties and the inability to manufacture those materials to the proper dimensions.

Current glaucoma drainage devices are constructed from materials with a long-standing history of use in tissue implantation. Materials for ophthalmic implantation have included stainless steel, titanium, silicone, and polypropylene.[28–30] However, both common metal and polymer materials have limitations, each lacking optimal dimensional and material properties for SC placement and long-term function. Traditional materials such as silicone demonstrate flexibility, whereas materials such as stainless steel exhibit rigidity for support; however, materials rarely combine both properties. Because of the unique and tiny circumferential anatomy of SC within the anterior chamber wall, a material that is superelastic yet maintains its structure is desirable.

Nitinol use in medical devices began in the 1970s.[31] Advantages of Nitinol, an alloy of 55% nickel and 45% titanium, include superelasticity, thermal shape memory behavior, high corrosive resistance, and biocompatibility.[32–37] These properties make Nitinol particularly suitable for use in applications requiring complex geometries, shape characteristics, and a circuitous delivery pathway; all conditions needed of a SC microstent. Because of its lack of cytotoxicity or mutagenic behavior, Nitinol recently has become a well-accepted alternative to traditional metallic and polymeric

Received for publication January 3, 2013; accepted August 27, 2013.
From the *Department of Eye and Vision Sciences, University of Liverpool, Liverpool, UK; †Department of Ophthalmology, McGill University, Montreal, QC; ‖Department of Ophthalmology and Visual Sciences, University of Toronto, Mississauga, ON, Canada; ‡Department of Ophthalmology, University of Colorado School of Medicine, Aurora, CO; §Department of Ophthalmology, University of Washington, Seattle, WA; #Department of Ophthalmology and Visual Sciences, University of Nebraska Medical Center, Omaha, NE; and ¶Ivantis Inc., Irvine, CA.
Supported by Ivantis Inc., and an unrestricted grant from Research to Prevent Blindness.
Disclosure: Andrew Schieber is employed by Ivantis. Malik Kahook consults for Glaukos. Murray Johnstone, Ike Ahmad and Ian Grierson consult for Ivantis.
Reprints: Carol B. Toris, PhD, Department of Ophthalmology and Visual Sciences, 985840 University of Nebraska Medical Center, Omaha, NE 68198-5840 (e-mail: ctoris@unmc.edu).

DOI: 10.1097/IJG.0000000000000012

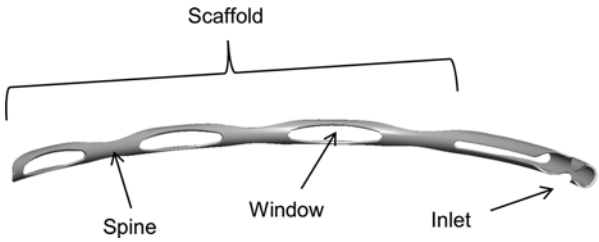

FIGURE 1. The Hydrus Microstent consists of scaffold to dilate Schlemm's canal and an inlet to bypass the trabecular meshwork.

biomaterials.[38–40] Nitinol has been used and tested in a number of locations in human and animal tissues, including the middle ear, cardiovascular system, the bladder, tendons, skin, bone, and the eye.[31,41–49] Although the intraocular use of Nitinol has been limited, preclinical studies with this material revealed that anterior chamber Nitinol clips were well tolerated at 10 weeks postoperatively.[49]

The current study evaluated the inflammatory response and biocompatibility of a novel SC Nitinol microstent (Hydrus Microstent; Ivantis Inc., Irvine, CA) in non-human primates (NHPs) and New Zealand white (NZW) rabbits.

MATERIALS AND METHODS

Test Article

The test article for both studies was a novel SC Nitinol microstent (Hydrus Microstent; Ivantis Inc., Fig. 1). The microstent has a scaffold region that dilates approximately 3 clock-hours of SC to provide increased circumferential flow of aqueous humor directly into multiple collector channels. The microstent also has an inlet that provides support to the opening through the TM by dilating SC, approximately 4 to 5 times the natural cross-sectional area (Fig. 2).

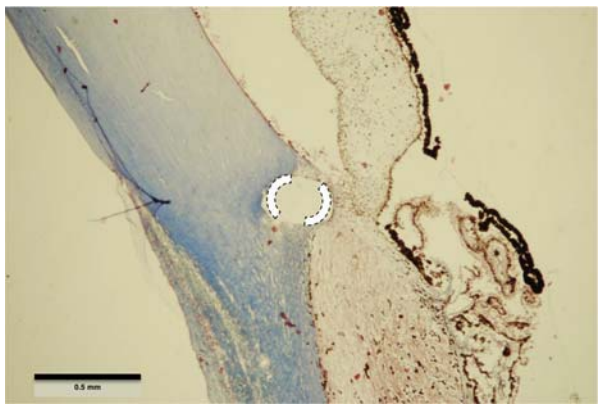

FIGURE 2. A cross-section of the Hydrus Microstent implanted postmortem in a non-human primate (NHP). The black dotted outline shows the location of microstent cross-section at the inlet region. This implant was positioned in the Schlemm's canal as a pilot feasibility assessment of the practicality of placement of the microstent in NHPs. Although implantation with the microstent was deemed feasible, it was noted that the NHP eyes were approximately 20% smaller than humans.

FIGURE 3. Hydrus Delivery System designed for ab interno microstent implantation into Schlemm's canal.

As with any implantable medical device, material processing is critical to ensure a biocompatible surface.[49,50] To enhance biocompatibility, the microstents were electropolished to passivate the surface and replace corrosive metallic elements with a nonreactive titanium oxide layer.[50–52] Testing was performed to verify the presence of the oxide layer and corrosion resistance of the implant surface.[53] Electropolishing removed sharp edges and provided a smooth uniform surface to minimize tissue reaction. The microstents were inspected using scanning electron microscopy (SEM) to ensure that the surface and edges were smooth and uniform.

The microstent was preloaded in a delivery system (Fig. 3) designed for placement through a corneal incision permitting ab interno implantation into SC under gonioscopic visualization. The cannula tip was designed to facilitate entry through the TM into SC. Once in the canal, the microstent was advanced and released from the delivery system under continued gonioscopic visualization. For anatomic reasons the delivery methods in the current study differed from the approach used in humans. All test articles (Hydrus Microstents) were sterilized before implantation.

ANIMAL STUDIES

Institutional Animal Care and Use Committee approval was obtained before initiation of any animal study. All animals were housed according to the Guide for the Care and Use of Lab Animals.[54] Animals were checked daily for mortality and morbidity. All applicable portions of the study conformed to the (OPRR), "Public Health Service Policy on Humane Care and Use of Laboratory Animals."[55,56]

Primate Study

Studies were conducted in 3 male mature adult cynomolgus NHPs (*Macaca fascicularis*) between 7 and 8 years of age. Two NHPs had a unilateral SC implant of the microstent and 1 had a unilateral sham surgery as the control. An ophthalmic surgeon experienced in similar procedures performed the surgeries and follow-up examinations were carried out by a board-certified veterinary ophthalmologist. The preoperative ocular evaluation included a slit-lamp examination, indirect ophthalmoscopy, and IOP measurements. A portable Tonopen was used to measure IOP in each eye with the 95% confidence interval readings recorded. The same examination was performed at

1 day after surgery and then at approximately 2, 4, 8, and 13 weeks.

Implantation Procedure

Before this study, the procedure was perfected using ex vivo eyes harvested from a cynomolgus NHP. Although the NHP was deemed a suitable animal model for SC microstent implantation, NHP eyes are approximately 20% smaller than those of humans (Fig. 2). The test articles were designed for human eyes and were thus slightly oversized for the NHP eye. Therefore, it was anticipated that this study would demonstrate a worse case for mechanical tissue stretching and compression.

Microstent implantation was conducted under general anesthesia. The eye was prepped and draped in the usual sterile manner. The eye was rotated downward to expose the superior conjunctiva. A traction suture of 4-0 silk passed through the superior rectus to permit eye fixation. A superior conjunctival peritomy was performed to expose bare sclera. Hemostasis was achieved with a low temperature battery cautery. A scleral flap was created with a micro-knife, and SC was unroofed. Once the canal was identified and dilated with Healon (an ophthalmic viscoelastic device), the microstent was implanted. An ab externo approach was used in the NHP eyes; therefore, the microstent implantation did not require use of the delivery system developed for the ab interno approach in human eyes. With smooth tipped forceps, the microstent was gently inserted into the exposed SC. An incision was made through the TM and 1 mm of the inlet was pushed into the anterior chamber. The scleral flap and conjunctiva were closed with an 8-0 Vicryl suture. The procedure for the sham was exactly the same, except the microstent was omitted.

Histologic Evaluation

The animals were euthanized at 13 weeks, the eyes enucleated, and the surgical sites prepared for evaluation by microscopy. Sutures were placed both near the insertion site and the distal end of the microstent to mark the location. The eyes were then immersion fixed in a solution consisting of 8 mL of glutaraldehyde, 20 mL formaldehyde, and 72 mL 0.1 M Sorensen's Phosphate Buffer.

Two NHP globes underwent histologic sectioning. The control animal globe was prepared using standard paraffin techniques. Because of the presence of the microstent in the experimental eye, plastic embedding with Spurr resin and surface polishing of thick sections was needed to obtain images of the microstent in situ. The thick sections were then cut serially every 0.5 to 1 mm into 15 plastic wafers. Thick wafers were sawn using a diamond saw (Exackt) and then ground and polished to a thickness between 60 and 80 μm for microscopic review. Either hematoxylin and eosin or Masson trichrome were used to stain the tissue sections, which were reviewed independently by the Department of Eye and Vision Science, University of Liverpool, UK and Lincoln Associates Inc., New Ipswich, NH. Encapsulation was assessed using the Jansen qualitative and semi-quantitative grading scheme for biocompatibility.[57] Thickness of fibroblast layers were scored from 1 to 4 by the Jansen scoring method with 4 the thinnest and 1 the thickest, typically well in excess of 30 fibroblast layers in thickness.

The third NHP globe underwent examination by SEM. The microstent was lifted out of SC, before tissue preparation, leaving a slit opening in the canal floor. Under a dissecting microscope, the microstent was inspected for debris and fibrin formation. In addition, the canal opening was carefully widened to expose the external wall of SC and regional collector channel ostia. The tissues were prepared for SEM using dehydration and gold sputter coating.

Examination of the microstent insertion point, area of passage, most distal extension, SC external wall, and collector channel ostia was done by SEM. Comparisons were made between regions of SC in which the microstent was implanted and adjacent nonimplanted regions; the presence of irregular particulate debris was noted and tissue damage was recognized by the presence of irregular surfaces.

Rabbit Study

Eight female NZW adult rabbits weighing 4.2 to 5.0 kg underwent Hydrus Microstent implantation. Follow-up slit-lamp examinations and photographs were conducted at 1, 2, and 4 weeks and 2, 4, and 6 months postsurgery. Ocular changes were scored according to the Hackett and McDonald's Ocular Scoring System.[58]

Implantation Procedure

The microstent was implanted in contact with a sampling of tissues including sclera, orbital tissues, and the conjunctiva. Placement within the subconjunctival space was an attempt to provide a worse case challenge for the presence of an inflammatory response.[59] Each animal was sedated with general anesthesia before surgery. Surgery was performed in the right eye for the microstent implant and the left eye for the sham surgery. Injection of balanced salt solution under the conjunctiva was performed to prevent penetration of the conjunctiva during implantation. The Hydrus Microstent was delivered through the cannula which was advanced initially through the cornea and across the anterior chamber, through the angle and into the subconjunctival space (Fig. 4). The cannula then was retracted slightly leaving 1 to 2 mm of the proximal end of the microstent in the anterior chamber. The delivery cannula then was removed from the eye and the anterior chamber was reformed to full depth with balanced salt solution. In 1 eye, the cannula entered the interior of the eye through the thin sclera. In the remaining eyes, the microstents were in

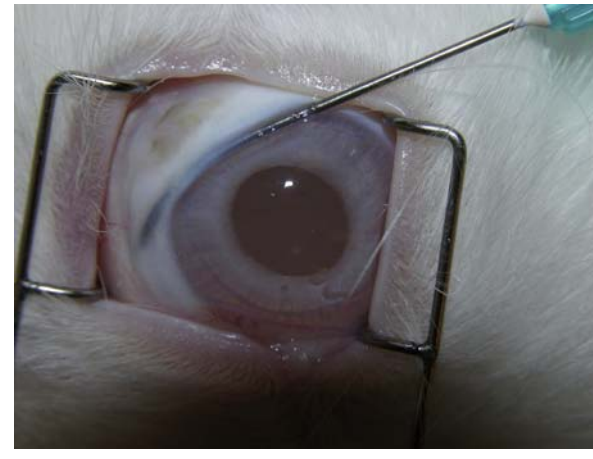

FIGURE 4. Cannula positioned in the rabbit eye through the cornea and across the anterior chamber, through the angle and into the subconjunctival space and orbital muscle.

contact with mostly orbital tissues. A sham procedure without the microstent was performed in the fellow eye of each animal. A topical ophthalmic antibiotic ointment (tobramycin) was applied 3 times daily for 48 hours. A veterinary ophthalmic surgeon experienced in similar implantation procedures performed the surgeries.

Histologic Evaluation

At 6 months after implantation, the animals were euthanized. Two sutures were placed in the cornea of each eye bordering the implant site. Both eyes from each animal were enucleated and immersed in a solution of Davidson's fixative for 18 to 24 hours at which time the eyes were rinsed with 70% ethanol and then immersed in fresh 70% ethanol for shipment. The eyes were processed by embedding experimental eyes in plastic and sham controls in paraffin, then sectioned and stained with hematoxylin and eosin. A qualified pathologist evaluated the optic nerve, choroid, retina, ciliary body, lens, cornea, and posterior and anterior chambers by ocular histopathologic examination.

The tissues adjacent to the microstent were examined for typical reactions to metallic materials, inflammatory response, giant cell presence, and microstent encapsulation. Encapsulation was assessed using the Jansen qualitative and semiquantitative grading scheme for biocompatibility.[57] The grading scheme highlights the reaction zone around the microstent and its interstices. In Jansen scoring, 4 is the thinnest capsule and 1 the thickest, typically well in excess of 30 fibroblast layers in thickness. The histopathologic evaluation was performed by Colorado Histo-Prep, Fort Collins, CO, and the evaluation of local reaction was conducted in the Department of Eye and Vision Science, University of Liverpool, UK.

RESULTS AND OBSERVATIONS

Primate Study

The in vivo clinical examinations during the 90-day term of this study did not demonstrate any abnormalities; IOP was within a normal range at all observation intervals.

Histologic Evaluation

Tissue appearance in the area of the microstent varied from partial loss of the TM tissue volume to loss of recognizable features of the TM and SC likely as a result of tissue compression associated with the presence of the microstent within SC (Fig. 5). Despite mechanical compression, the host response to the microstent within the ocular tissues at the anterior angle was judged to be minimal. For example, there was no evidence of tissue degeneration adjacent to the microstent or elsewhere within the eyes. No histopathologic evidence of metallosis such as depigmentation, apoptosis, or tissue necrosis was present. The host response to the implanted microstent was the presence of a few mononuclear cells with no marked granulomatous response and an absence of giant cells in the adjacent tissue (Fig. 5). No significant inflammatory process was seen. A low-grade mononuclear response involving a few scattered macrophages was present in some tissues both close to and remote from the microstent. Encapsulation was difficult to assess except in areas adjacent to the empty space at the site where the microstent section was dislodged during processing. In the tissue surrounding the empty space, an extremely thin capsule wall could be seen

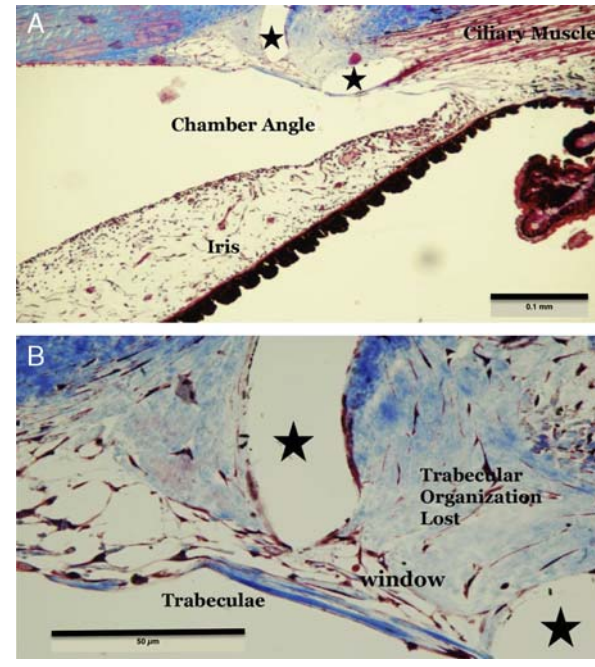

FIGURE 5. A, A cross-section of an experimental non-human primate (NHP) eye with the region in which the Hydrus Microstent had been contained (black stars). B, Higher magnification of a NHP cross-section of microstent region (black stars) with the presence of a few mononuclear cells with no marked granulomatous response and an absence of giant cells in the adjacent tissue. Close examination of the capsule showed a lack of any substantial fibrous collagen component.

consisting of 1 to 2 thin spindle-shaped fibroblasts. The capsule thickness was scored 4 on the Jansen biocompatibility score for reaction zone size. Close examination of the capsule showed a lack of any substantial fibrous collagen component (Fig. 5).

Ninety days after implantation, SEM examination demonstrated the Hydrus Microstent within SC (Fig. 6) and the inlet of the microstent located in the anterior chamber. The microstent had clearly stretched and the TM and enlarged SC (Fig. 6). With removal of the microstent, SC appeared patent (Fig. 7). The limited host response, as noted with light microscopy, was observed at the external surface of the microstent with SEM. The channel of the microstent was patent (Fig. 8). There were no changes noted with SEM on the surface of the microstent.

Rabbit Study

In vivo examinations during the 6-month term of this study did not demonstrate any significant morbidity from the microstents. Ophthalmic abnormalities observed in this study included a low-grade anterior uveitis and bleeding resulting from the needle insertion into the anterior chamber. The uveitis and hyphema improved over a 2-week period and had completely resolved by the 4-week examination. From 4 weeks until the conclusion of the 6-month study, both the sham and the experimental eyes were quiet with no visible abnormalities identified.

Histologic Evaluation

Histopathologic examination of the sham-operated eyes allowed the identification of the surgical wound site

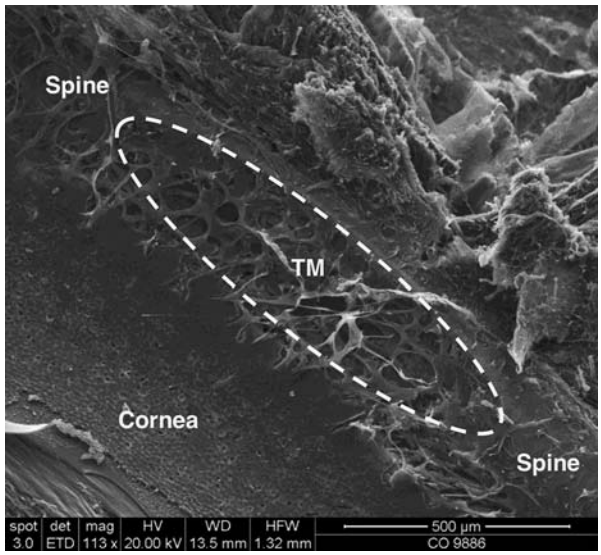

FIGURE 6. A scanning electron microscopy image of the microstent in Schlemm's canal of a non-human primate eye. The microstent had been in the eye for 90 days. A window of the microstent with trabecular meshwork (TM) stretched across is outlined by the white dotted line.

extending through ocular tissues, forming a subconjunctival pocket and sometimes entering orbital tissue. The repaired wound sites were unremarkable except for small foci of inflammatory mononuclear cells particularly in the region of the conjunctiva (Fig. 9). Occasional isolated giant cells were found (between 0 and 2 per section) in orbital and intraocular locations (Fig. 10).

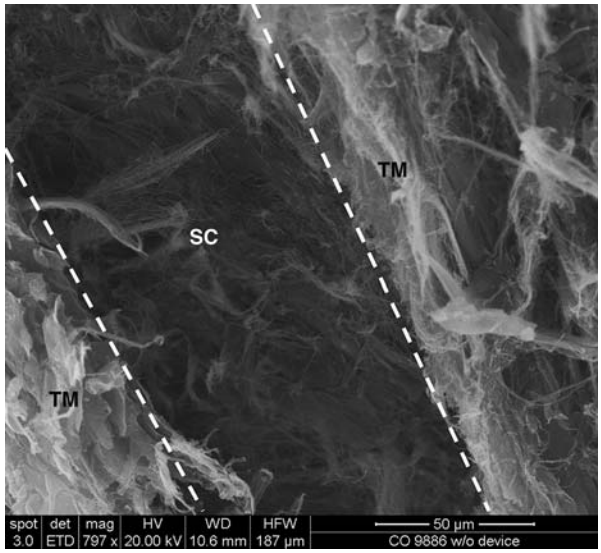

FIGURE 7. A scanning electron microscope image of the trabecular meshwork (TM) and Schlemm's canal (SC) of a non-human primate after the Hydrus Microstent had been lifted out leaving the external wall exposed. SC is marked with 2 white dotted lines surrounded by TM remnants. This is the same eye as in Figure 6. There was no evidence of an acute or chronic inflammatory response, granulation response, or fibrosis in or around the canal.

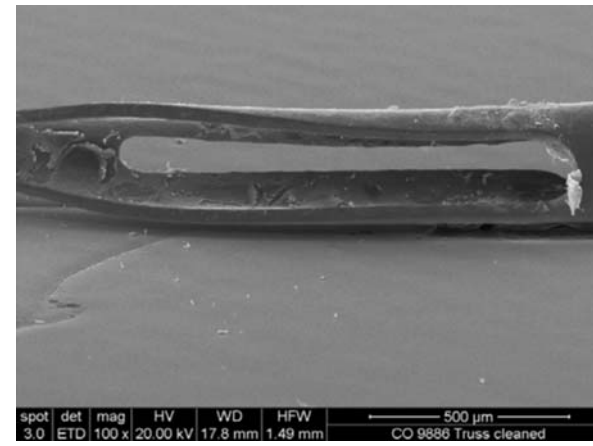

FIGURE 8. The window and channel of a microstent after removal from a non-human primate. The surface of the microstent was covered with a thin layer of tissue but otherwise was surprisingly clean after having been in the Schlemm's canal for 3 months.

In 1 experimental eye, the sectioned microstent was not identified for technical reasons. In another experimental eye, the microstent was noted to have entered the sclera and ciliary body. In all the other experimental eyes, the implantation location was primarily in orbital and extraocular tissues including extraocular muscle, orbital fat, orbital connective tissue, and conjunctiva. Degenerative changes, necrosis, or apoptosis were not seen in orbital, extraocular, or intraocular tissue. Inflammatory cells were seldom present within tissues remote from the microstent. Scattered mononuclear cells were present in the tissues directly surrounding the microstent in all 7 specimens where the microstent was identified. The inflammatory cells surrounding the microstent were infrequent and were mostly macrophages. Although florid granulomatous tissue was not seen anywhere, a few small, isolated giant cells were identified in the orbital tissue of 2 specimens; in 3 specimens there was 1 giant cell per section, and in the others none were seen.

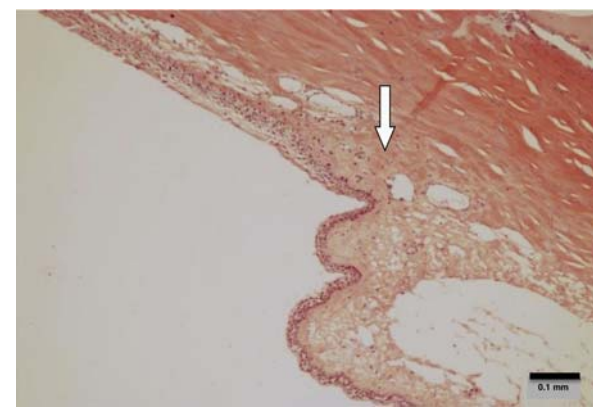

FIGURE 9. The sham-operated control eye of a rabbit demonstrating a low-grade monocytic cell response (white arrow) still active in front of the pocket at the conjunctival and superficial limbal junction and at the limit of the limbal vascular arcades.

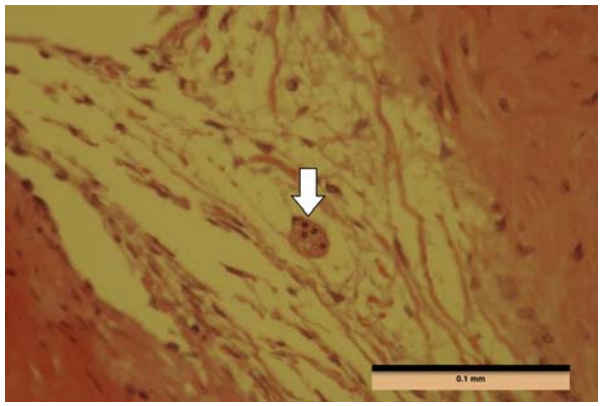

FIGURE 10. Sham-operated control eye from a rabbit. There is a giant cell (white arrow) within the trabecular meshwork, close to the aqueous plexus.

Encapsulation of the implanted microstent with fibroblasts was minimal and difficult to appreciate except in en face or oblique sections (Figs. 11–13). In 1 specimen the reaction zones of the capsule reached a grade 3 Jansen thickness score, 6 layers of fibroblasts in the thickest part of the capsule. The remaining specimens had a grade 4 Jansen thickness score with a maximum of 1 to 3 fibroblast layers.

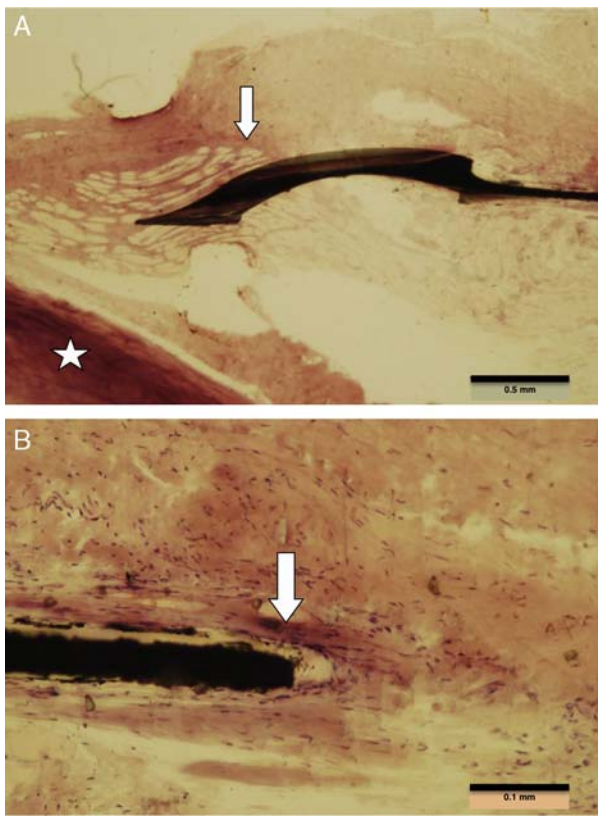

FIGURE 11. The microstent is sectioned for a substantial length in the orbital tissues (white arrow) as seen in (A) where the sclera is indicated by a white star. B, Part of the microstent at high power where the capsule (white arrow) is most apparent although it represents a minor tissue reaction.

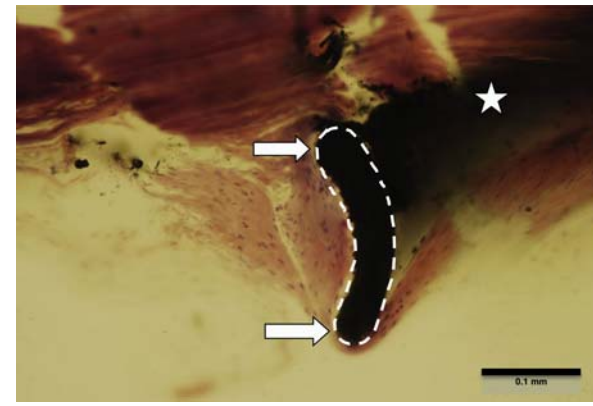

FIGURE 12. The microstent highlighted with a white dotted outline within the sclera (white star) and extends through the coats of the eye (white arrows) into the interior of a rabbit eye. There is minimal capsule formation, very few macrophages, and no other inflammatory cells associated with the microstent.

Oblique (Fig. 11) and en face (Fig. 13) views of these insubstantial capsules demonstrated that even the most developed capsules did not have a pronounced, fibrous

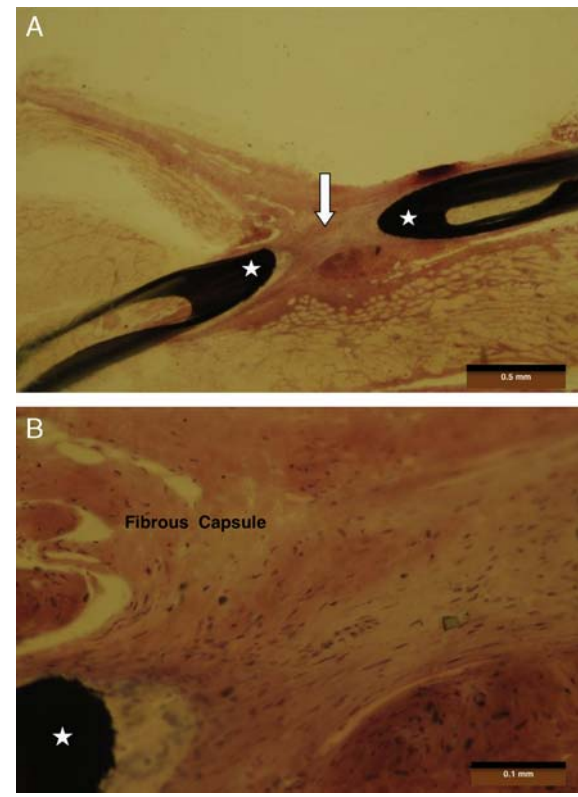

FIGURE 13. Microstent in the orbital tissue of an experimental rabbit eye. A, Two segments of the microstent (white stars) and a region of fibrous repair tissue seen in flat to oblique section (en face) marked with a white arrow. The fibrous capsule is seen at higher magnification in (B) with the left hand segment of the Hydrus microstent identified as the black structure (white star). The fibrous capsule is seen in bird's eye view and appears relatively inert.

extracellular matrix component nor were the capsules heavily infiltrated with inflammatory cells. The numbers of inflammatory cells around the microstent were only marginally more frequent than those found at the sites of the sham operations. Although a few giant cells were noted in most of the experimental eyes, 1 or 2 giant cells were also found in the sections from sham-operated controls.

DISCUSSION

The Hydrus Microstent was assessed for biocompatibility by extended in vivo follow-up studies in both NHP and rabbit eyes. Assessment by light microscopy and SEM revealed minimal inflammation. It appears from these preclinical studies that the Hydrus Microstent has properties to provide excellent long-term biocompatibility.

An important therapeutic goal for the reduction of IOP is to develop devices that increase facility of aqueous humor outflow through the conventional aqueous humor outflow system. Although surgical techniques to achieve the goal are well known, implantation within SC is limited by the physical properties of available biomaterials. Recent applications of Nitinol-based devices, most notably within the cardiovascular system, suggested there might be similar benefits in ophthalmologic applications.[40–49] However, the host response of the eye to Nitinol has been described only once previously.[49]

The present study assessed biocompatibility of a Nitinol-based Hydrus Microstent processed with a passive titanium oxide layer. The in vivo study conducted for up to 6 months in rabbits and 90 days in NHPs demonstrated a minimal host response in terms of inflammatory cell infiltrate, giant cell formation, or microstent fibrotic encapsulation. The inflammatory cells in both NHP and rabbit consisted of only a few scattered mononuclear cells mostly macrophages surrounding the device with none seen in locations remote from the device.

Evidence of an initial or late acute or chronic inflammatory response was absent. In fact, the numbers of inflammatory cells around the microstent in the rabbits were only marginally more frequent than those found at the sites of the sham operations. The paucity of giant cells in association with the microstent in both NHP and rabbits provided further evidence of minimal inflammatory activity. The incidence of inflammatory cells per unit area at each of the key sites where inflammatory cells were found was so low that meaningful effort at quantitation was not attempted. The "noise" levels would have rendered comparative counts on the limited number of sections meaningless. Although a few giant cells were noted in most of the experimental rabbit eyes, 1 or 2 giant cells also were found in the sections from sham-operated controls. Collagen is usually prominent in the reactive zone of the thick capsule surrounding poorly biocompatible materials.[60] However, in this study both the NHP and the rabbits had minimal collagenous encapsulation of the microstent. In fact, in many examples the capsule was difficult to see except in oblique section where it was evident that the capsules consisted of a few spindle-shaped fibroblasts and a paucity of extracellular materials including collagen.

It might be predicted that the Hydrus Microstent positioned within the relatively avascular region of the outflow system of the NHP eye would exhibit a minimal inflammatory response. Minimal inflammatory reaction was found, even with 90 days of chronic exposure. In contrast, the microstent was lodged in highly vascularized and highly reactive tissues of the rabbit eyes including orbital tissue, extraocular muscle, and conjunctiva for 6 months providing a much more rigorous test of biocompatibility. Even with the more extreme tissue challenge, the microstent provoked little in the way of a cellular reaction.

Rabbits are a species renowned for the vigor of their ocular injury sensitivity.[57,59] With this in mind, the minimal response to Nitinol in the biologically reactive tissues of the species is reassuring. In comparison with the responses to other biomaterials utilized for ophthalmologic implantation, such as silicone the host response to Nitinol was found to be quite limited.[28] The host response to Nitinol was no greater than expected of that with materials such as polypropylene or collagen.[29] Perhaps the inflammatory response of the Hydrus Nitinol microstent was reduced partly because the microstent is quite small and exhibits superelasticity allowing the microstent to conform to the implantation site. The inflammatory response to Nitinol is similar to materials such as stainless steel, another material widely used for fabrication of biomedical implants.[30] However, both the physical characteristics of Nitinol, such as shape memory and superelasticity confer benefits to Nitinol not available with stainless steel implants.

In summary, the unique physical features of shape memory alloy devices constructed of Nitinol appear ideally suited for the minimally invasive surgical needs of the outflow system of the eye. In this study, long-term implantation of the Hydrus Microstent in NHP and NZW rabbit eyes demonstrated the biocompatibility of implants fabricated from Nitinol for intraocular implantation. These studies suggest that clinical evaluation of the Hydrus Microstent can be conducted with an expectation of no significant inflammatory response or fibrotic encapsulation.

ACKNOWLEDGMENTS

The authors thank Steven Grosser, MD; Stephen Bistner, DVM, DACVO; and Randy White, PhD for providing animal eye examinations, surgeries, and study direction.

REFERENCES

1. Gedde SJ, Schiffman JC, Feuer WJ, et al. Treatment outcomes in the tube versus trabeculectomy (TVT) study after five years of follow-up. *Am J Ophthalmol*. 2012;153:789–803.
2. Gedde SJ, Schiffman JC, Feuer WJ, et al. Treatment outcomes in the tube versus trabeculectomy study after one year of follow-up. *Am J Ophthalmol*. 2007;143:9–22.
3. Gedde SJ, Schiffman JC, Feuer WJ, et al. Three-year follow-up of the tube versus trabeculectomy study. *Am J Ophthalmol*. 2009;148:670–684.
4. Radcliffe NM, Musch DC, Niziol LM, et al. The effect of trabeculectomy on intraocular pressure of the untreated fellow eye in the Collaborative Initial Glaucoma Treatment Study. *Ophthalmology*. 2010;117:2055–2060.
5. The AGIS Investigators. The Advanced Glaucoma Intervention Study (AGIS): 9. Comparison of glaucoma outcomes in black and white patients within treatment groups. *Am J Ophthalmol*. 2001;132:311–320.
6. Gedde SJ, Herndon LW, Brandt JD, et al. Postoperative complications in the tube versus trabeculectomy (TVT) study during five years of follow-up. *Am J Ophthalmol*. 2012;153:804–814.
7. Francis BA, Singh K, Lin SC, et al. Novel glaucoma procedures. *Ophthalmology*. 2011;118:1466–1480.

8. Saheb H, Ahmed IK. Micro-invasive glaucoma surgery: current perspectives and future directions. *Curr Opin Ophthalmol*. 2012;23:96–104.
9. Rosenquist R, Epstein D, Melamed S, et al. Outflow resistance of enucleated human eyes at two different perfusion pressures and different extents of trabeculotomy. *Curr Eye Res*. 1989;8:1233–1240.
10. Ellingsen BA, Grant WM. Influence of intraocular pressure and trabeculotomy on aqueous outflow in enucleated monkey eyes. *Invest Ophthalmol*. 1971;10:705–709.
11. Ellingsen BA, Grant WM. Trabeculotomy and sinusotomy in enucleated human eyes. *Invest Ophthalmol*. 1972;11:21–28.
12. Minckler DS, Hill RA. Use of novel devices for control of intraocular pressure. *Exp Eye Res*. 2009;88:792–798.
13. Francis BA, Minkler DS, Dustin L, et al. Combined cataract extraction and trabeculotomy by the internal approach for coexisting cataract and open-angle glaucoma: initial results. *J Cataract Refract Surg*. 2008;34:1096–1103.
14. Minckler D, Mosaed S, Dustin L, et al. Trabectome (trabeculectomy-internal approach): additional experience and extended follow-up. *Trans Am Ophthalmol Soc*. 2008;106:149–160.
15. Mosaed S, Dustin L, Minckler DS. Comparative outcomes between newer and older surgeries for glaucoma. *Trans Am Ophthalmol Soc*. 2009;107:127–133.
16. Philippin H, Wilmsmeyer S, Feltgen N, et al. Combined cataract and glaucoma surgery: endoscope-controlled erbium:YAG-laser goniotomy versus trabeculectomy. *Graefes Arch Clin Exp Ophthalmol*. 2005;243:684–688.
17. Johnstone MA, Grant WM. Microsurgery of Schlemm's canal and the human aqueous outflow system. *Am J Ophthalmol*. 1973;76:906–917.
18. Johnson MC, Kamm RD. The role of Schlemm's canal in aqueous outflow from the human eye. *Invest Ophthalmol Vis Sci*. 1983;24:320–325.
19. Johnson M. What controls aqueous humour outflow resistance? *Exp Eye Res*. 2006;82:545–557.
20. Grant WM. Experimental aqueous perfusion in enucleated human eyes. *Arch Ophthalmol*. 1963;69:783–801.
21. Murphy CG, Johnson M, Alvarado JA. Juxtacanalicular tissue in pigmentary and primary open angle glaucoma. The hydrodynamic role of pigment and other constituents. *Arch Ophthalmol*. 1992;110:1779–1785.
22. Grant WM. Clinical measurements of aqueous outflow. *Arch Ophthalmol*. 1951;46:113–131.
23. Bahler CK, Smedley GT, Zhou J, et al. Trabecular bypass stents decrease intraocular pressure in cultured human anterior segments. *Am J Ophthalmol*. 2004;138:988–994.
24. Bahler CK, Hann CR, Fjield T, et al. Second-generation trabecular meshwork bypass stent (iStent inject) increases outflow facility in cultured human anterior segments. *Am J Ophthalmol*. 2012;153:1206–1213.
25. Samuelson TW, Katz LJ, Wells JM, et al. Randomized evaluation of the trabecular micro-bypass stent with phacoemulsification in patients with glaucoma and cataract. *Ophthalmology*. 2011;118:459–467.
26. Dietlein TS, Friedrich J, Schild A, et al. Combined cataract-glaucoma surgery using the intracanicular eyepass glaucoma implant, first clinical results of a prospective pilot study. *J Cataract Refract Surg*. 2008;34:247–252.
27. Camras LJ, Yuan F, Fan S, et al. A novel Schlemm's canal scaffold increases outflow facility in a human anterior segment perfusion model. *Invest Ophthalmol Vis Sci*. 2012;53:6115–6121.
28. Ayyala RS, Harman LE, Michelini-Norris B, et al. Comparison of different biomaterials for glaucoma drainage devices: part 1. *Arch Ophthalmol*. 1999;117:233–236.
29. Ayyala RS, Michelini-Norris B, Flores A, et al. Comparison of different biomaterials for glaucoma drainage devices: part 2. *Arch Ophthalmol*. 2000;118:1081–1084.
30. Nyska A, Glovinsky Y, Belkin M, et al. Biocompatibility of the Ex-PRESS miniature glaucoma drainage implant. *J Glaucoma*. 2003;12:275–280.
31. Castleman LS, Motzkin SM, Alicandri FP, et al. Biocompatibility of Nitinol alloy as an implant material. *J Biomed Mater Res*. 1976;10:695–731.
32. Henderson E, Nash DH, Dempster WM. On the experimental testing of fine Nitinol wires for medical devices. *J Mech Behav Biomed*. 2011;4:261–268.
33. Haider W, Munroe N. Assessment of corrosion resistance and metal ion leaching of Nitinol alloys. *J Mater Eng Perform*. 2011;20:812–815.
34. Haider W, Munroe N, Pulletikurthi C, et al. A comparative biocompatibility analysis of ternary Nitinol alloys. *J Mater Eng Perform*. 2009;18:760–764.
35. Venugopalan R, Trepanier C. Assessing the corrosion behaviour of Nitinol for minimally-invasive device design. *Min Invas Ther Allied Technol*. 2000;9:67–74.
36. Shabalovskaya SA. Surface, corrosion and biocompatibility aspects of Nitinol as an implant material. *Biomed Mater Eng*. 2002;12:69–109.
37. Trepanier C, Venugopalan R, Pelton AR. Corrosion resistance and biocompatibility of passivated NiTi. In: Yahia L, ed. *Shape Memory Implants*. New York: Springer; 2000:35–45.
38. Assad M, Chernyshov A, Leroux MA, et al. A new porous titanium-nickel alloy: part 1. Cytotoxicity and genotoxicity evaluation. *Biomed Mater Eng*. 2002;12:225–237.
39. Bombac D, Brojan M, Fajfar P, et al. Review of materials in medical applications. *Mater Geoenviron*. 2007;54:471–499.
40. Hannula SP, Söderberg O, Jämsä T, et al. Shape memory alloys for biomedical applications. *Adv Sci Technol*. 2006;49:109–118.
41. Roosli C, Schmid P, Huber AM. Biocompatibility of nitinol stapes prosthesis. *Otol Neurotol*. 2011;32:265–270.
42. Achneck HE, Jamiolkowski RM, Jantzen AE, et al. The biocompatibility of titanium cardiovascular devices seeded with autologous blood-derived endothelial progenitor cells: EPC-seeded antithrombotic Ti implants. *Biomaterials*. 2011;32:10–18.
43. Verheye S, De Meyer G, Salu K, et al. Histopathologic evaluation of a novel-design nitinol stent: the Biflex stent. *Int J Cardiovasc Interv*. 2004;6:13–19.
44. Hill AC, Maroney TP, Virmani R. Facilitated coronary anastomosis using a nitinol U-Clip device: bovine model. *J Thorac Cardiovasc Surg*. 2001;121:859–870.
45. Balakrishnan N, Uvelius B, Zaszczurynski P, et al. Biocompatibility of nitinol and stainless steel in the bladder: an experimental study. *J Urol*. 2005;173:647–650.
46. Kujala S, Pajala A, Kallioinen M, et al. Biocompatibility and strength properties of Nitinol shape memory alloy suture in rabbit tendon. *Biomaterials*. 2004;25:353–358.
47. Wever DJ, Veldhuizen AG, Sanders MM, et al. Cytotoxic, allergic and genotoxic activity of a nickel-titanium alloy. *Biomaterials*. 1997;18:1115–1120.
48. Beeley NRF, Stewart JM, Tano R, et al. Development, implantation, in vivo elution, and retrieval of a biocompatible, sustained release subretinal drug delivery system. *J Biomed Mater Res*. 2006;76:690–698.
49. Olson JL, Velez-Montoya R, Erlanger M. Ocular biocompatibility of Nitinol intraocular clips. *Invest Ophthalmol Vis Sci*. 2012;53:354–360.
50. Shabalovskaya SA, Anderegg J, Van Humbeeck J. Critical overview of Nitinol surfaces and their modifications for medical applications. *Acta Mater*. 2008;4:447–467.
51. Shabalovskaya SA, Tian H, Anderegg JW, et al. The influence of surface oxides on the distribution and release of nickel from Nitinol wires. *Biomaterials*. 2009;30:468–477.
52. Shabalovskaya SA. On the nature of the biocompatibility and on medical applications of NiTi shape memory and superelastic alloys. *Biomed Mater Eng*. 1996;6:267–289.
53. Wever DJ, Veldhuizen AG, De Vries J, et al. Electrochemical and surface characterization of a nickel-titanium alloy. *Biomaterials*. 1998;19:761–769.
54. Grossblatt N. *Guide for the Care and Use of Lab Animals*. Washington, DC: National Academy Press; 1996.

55. Health Research Extension Act of 1985 (Public Law 99-158), Revised 1986. Available at: http://grants.nih.gov/grants/olaw/references/hrea1985.htm.
56. USDA, Department of Agriculture, Animal and Plant Health Inspection Service, 9 CFR, Parts 1, 2, and 3, Animal Welfare, Final Rule 1989. Available at: http://grants.nih.gov/grants/olaw/references/phspolicylabanimals.pdf.
57. Wilhelmus K. The Draize eye test. *Surv Ophthalmol*. 2001;45:493–515.
58. Hackett RB, McDonald TO. Assessing ocular irritation. In: Marzulli FN, Maibach HI, eds. *Dermotoxicity*. Washington, DC: Hemisphere Publishing; 1996:557–567.
59. Bito LZ, Klein EM. The unique sensitivity of the rabbit eye to x-ray-induced ocular inflammation. *Exp Eye Res*. 1981;33:403–412.
60. Jansen JA, Dhert WJ, Van Der Waerden JP, et al. Semi-quantitative and qualitative histologic analysis method for the evaluation of implant biocompatibility. *J Invest Surg*. 1994;7:123–134.